25.1: ARROW-Based Optical Accelerometers

A. Llobera
Centro Nacional de Microelectrónica Campus UAB, Cerdanyola del Vallés, Barcelona, Spain
Andreu.llobera@cnm.es

J. A. Plaza
Centro Nacional de Microelectrónica (CSIC), campus UAB, Cerdanyola del Vallés, Barcelona, Spain
joseantonio.plaza@cnm.es

I. Salinas
Dept. de Física Ap. Universidad de Zaragoza, 50009 Zaragoza, Spain
isalinas@posta.unizar.es

J. Berganzo
Ikerlan, Electronics and Components Deptartment, Spain
Jberganzo@ikerlan.es

J. Garcia
Ikerlan, Electronics and Components Deptartment, Spain
Jberganzo@ikerlan.es

J. Esteve
Centro Nacional de Microelectrónica (CSIC), campus UAB, Cerdanyola del Vallés, Barcelona, Spain
Jaume.esteve@cnm.es

C. Domínguez
Centro Nacional de Microelectrónica (CSIC), campus UAB, Cerdanyola del Vallés, Barcelona, Spain
carlos.dominguez@cnm.es

Abstract

Design, fabrication and characterization of silicon-based stress-free self-aligned quad beam accelerometer is presented. Standard total internal reflection waveguides have been replaced by ARROW structures, enhancing the sensitivity to >4dB/g at the wavelength visible range (633nm) Moreover, as the waveguide core has approximately the same size as the input fiber optic, insertion losses have been reduced to 2.5dB. Attenuation in ARROW waveguides is 0.3dB/cm.

Keywords

Optical Accelerometers, ARROW, Waveguides, MOEMS.

INTRODUCTION

Optical accelerometers are one of the most promising MOEMS structures in which much effort has been put since it can overcome the inherent piezoresitive/piezoelectric acceleroemeter problems. The capacitive accelerometers could require silicon-glass bonding so as to provide a narrow gap for the sensing capacitor [1] and suffer from inherent nonlinearity, as well as require an complicated electronic reading. Piezoelectric accelerometers produce a fairly linear output response with a relatively simple electronics, but are sensitive to temperature [2]. Moreover, none of the previously mentioned accelerometers is able to work under electromagnetic interference (EMI) [3] or having the supply sources far away from the device without causing much noise on the output reading. Thus, optical accelerometers are extremely useful in these application fields where its counterparts by no way can be used, as could be highly explosive atmospheres or under strong electromagnetic fields.

Up to date, there has been several proposals on the fabrication of optical accelerometers, using integrated optics [4] or fiber optics [5], being the latter the most common case for the shake of simplicity. Among the integrated optics accelerometers, the most widely employed consist in a silicon nitride total internal reflection (TIR) waveguide in cantilever configuration.

Silicon nitride can be obtained over any substrate using several deposition techniques, as could be Plasma Enhanced or Low Pressure Chemical Vapor Deposition (PECVD and LPCVD, respectively) and Sputtering. Each one provides the layer with different properties concerning its homogeneity, mechanical stress and even refractive index. Due to the better uniformity, step coverage and mechanical stability, LPCVD is normally chosen as the main deposition system for obtaining Si_3N_4 layers. Unfortunately, these films suffer from a high tensile stress that causes the structure to crack for thicknesses above 600nm. Although this dimension is by large enough for obtaining waveguides working in the visible range, it has to be taken into account the dimensions of the light source. If end-fire coupling is used, then light is coupled into the integrated optical device using a standard fiber optic, whose core has a diameter of 4μm. The large difference between the relative areas of both structures causes an extremely high insertion losses. Moreover, in order to assure cross-section light confinement, the core of integrated optical waveguides is partially etched, forming the so-called rib. In silicon nitride waveguides this rib seldom exceeds 50nm in size, being impossible to see it at naked eye and hardening the alignment. As far as the

optical accelerometer behavior in cantilever configuration is concerned, thin core also is a drawback. In figure 1a, total losses as a function of the waveguide misalignment is presented. As can be seen, although silicon nitride waveguides have very high sensitivity (since small misalignments cause an huge power variation at the output) the linear region (2nd derivate of the losses) where losses are directly proportional to acceleration changes (see figure 1b) is extremely small. Thence, optical accelerometers with waveguides of Si_3N_4 mostly act as a switch.

a)

b)
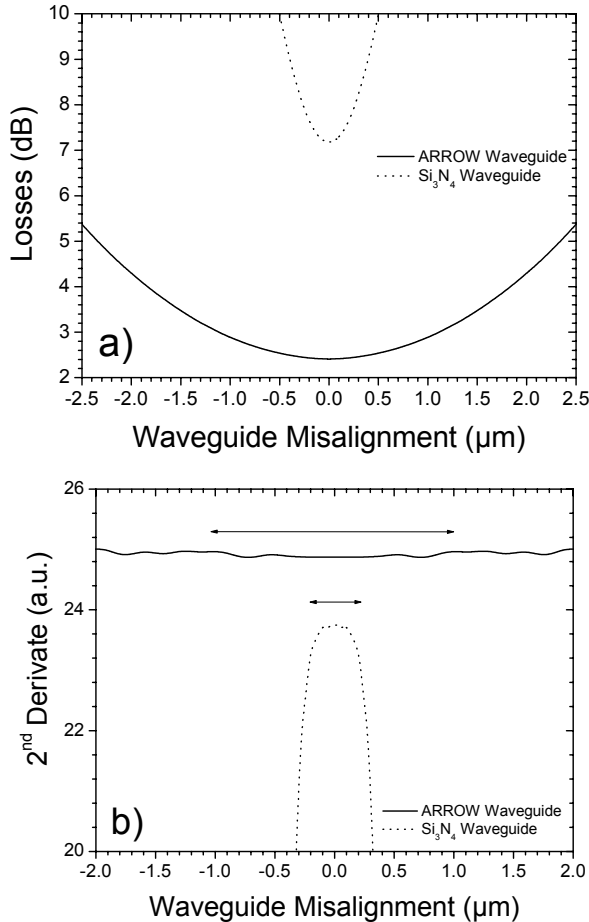
Figure 1. a) Total losses due to waveguide misalignment for 300nm-thick Si_3N_4 and ARROW waveguides. b) Linear regions where losses are directly proportional to misalignment. Waveguides are 30µm-separated

Another possibility with TIR waveguides would be the replacing of the silicon nitride by another material that did not have so strong mechanical stresses. Problems with this configuration arises with the substrate properties. Silicon has a high refractive index (3.85-i0.02 @0.633µm) and it is highly absorbent for wavelengths below 1.1µm. To overcome problems related to substrate (absorption or guiding for small or high wavelengths, respectively) what

is normally done is obtain a buffer layer over it, with lower refractive index than these of the core, that avoids light to tunnel from the core to the substrate. Unfortunately, in order to assure a complete core shielding, the buffer layers have to be very thick, that causes high stresses on the deposited layers.

Most of the previously mentioned drawbacks can be overcame if, instead of TIR configuration, another type of light confinement, the antiresonance, is used.

Antiresonant Reflecting Optical Waveguides (ARROW)**[6]** have received recently much attention due to its interesting properties. The basic configuration of an ARROW-A structure is presented in figure 2. Guiding in these waveguides is achieved via the Fabry Perot interferometer placed beneath the core. For a given working wavelength and for a fixed refractive index of the layers, there exist some values for d_1 and d_2 where a maximum reflection at the core-1st cladding boundary is observed (>99.96%) for the TE_0 **[7]**. At the upper core-air boundary, the guiding is caused by standard TIR. Higher order modes are filtered out since the antiresonant layers are not properly sintonized. Hence, this structure has monomode behavior for core thickness of the same size as the fiber optics, having much lower losses as compared to silicon nitride waveguides, as shown in figure 1a. Moreover, maybe the most important property that ARROW waveguides provide to the accelerometer design is the availability to work on a extremely wide linear range, as observed in figure 1b.
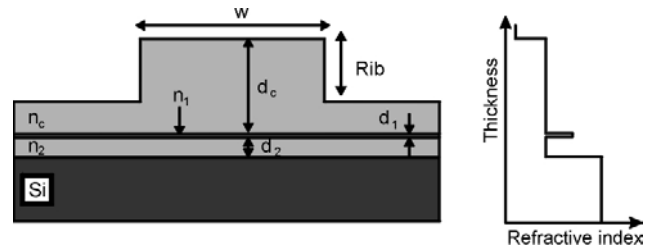
Figure 2. Standard configuration and refractive index profile of ARROW structures. The darker the Grey, the higher the refractive index is.

DESIGN & SIMULATION

On the basis of previously studied silicon-based ARROW waveguides **[8]** working in the visible range (λ=0.633µm) a new design for an optical accelerometer, as shown in figure 3, is proposed. It is a result from the combination of two opposite technologies: Integrated optics and MEMS. While the former demands for relatively thick layers so as to obtain good light confinement, the latter avoids as much as possible to have multilayer structures, in order not to have mechanical stresses or different thermal coefficients that could cause structure to bend. Agreement has been achieved having only waveguides in very concrete accelerometer regions, away from the bridges.
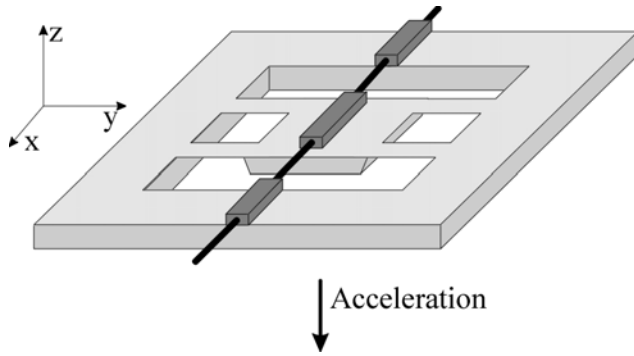
**Figure 3. Scheme of the Optical Accelerometer presented.**

It basically consists on a three-fold segmented waveguide. The input and output parts are placed on the chip frame, while the middle part is located over a quad-beam seismic mass. When the accelerometer suffers from an acceleration in the z direction, a double misalignment is produced, one at each cut. Distance between the seismic mass and frame has been chosen to be 24μm, which is the minimum necessary to have a properly defined structure, according to technological parameters. From an optical point of view, this distance should be as short as possible in order to avoid, as much as possible, pulse broadening. Nevertheless, maximum power transference between segments can be assured by ways of increasing the width at every step. Thus the first segment has w=14μm, the middle is 30μm width and the output segment has w=50μm.

Optical simulations of the total losses as a function of the segmented waveguide misalignment caused by the seismic mass displacement were done by the Non-Uniform Finite Difference Method (NU-FDM), together with the Beam Propagation Method (BPM). Figure 4 shows the propagating field across the accelerometer. When the three segments are aligned (figure 4a) the power at the output is the highest. If segments are progressively misaligned, both in +z or –z direction, the power at the output progressively decreases, as shown in figure 4b, when they are 2μm misaligned. It has to be noted that this self-aligned configuration also has a failure test, since if the accelerometer suffered an excessive acceleration that broke the seismic mass, power at the output will be the minimum, as seen in fig 4c.
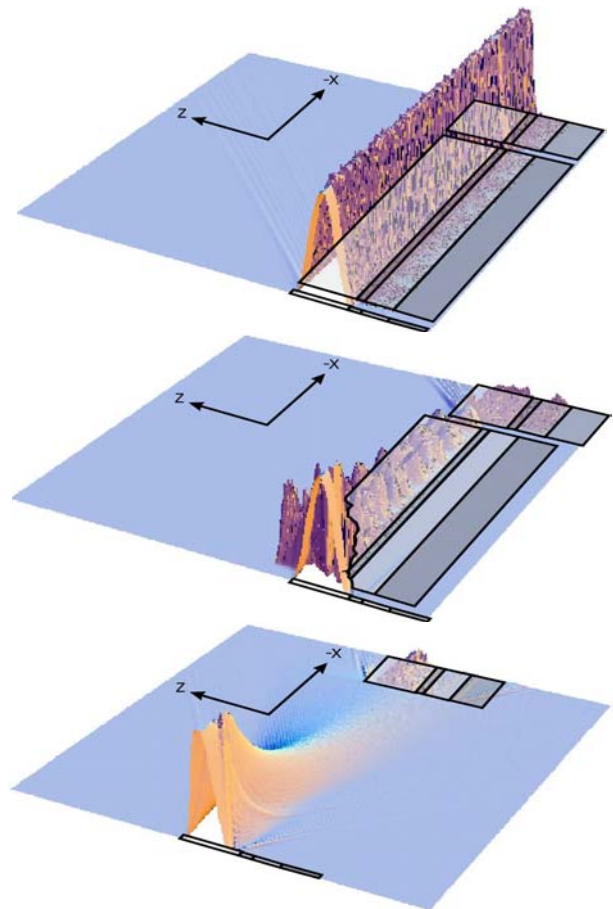
Figure 4. Propagating field on the optical accelerometer a) when all three segments are aligned. B) at 50% (2-μm) misaligned. c) without middle segment

Power at the segment output as a function of the seismic mass displacement (i.e. a double misalignment) without considering the insertion losses is presented in fig. 5. It is observed an expected symmetrical losses response depending on the sign of the displacement. What is more remarkable is the linear response over a large range that would allow the accelerometer to measure different speed changes.
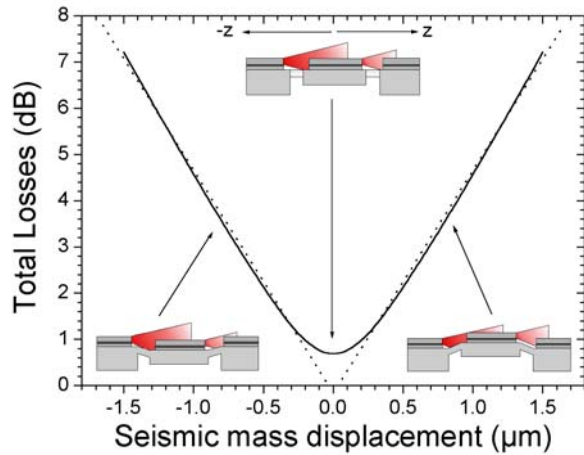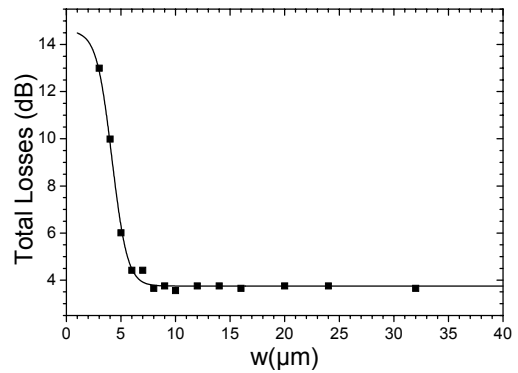
Figure 5. Total losses as a function of the seismic mass misalignment when considering the accelerometer configuration proposed.

Seismic mass displacement was chosen to range between 0 and 1μm. Although it is not the most optimum region, since around zero there exists a non-linear region, it has to be taken into account that a large seismic mass displacement causes stresses on the bridges, that may even broke them Once the working region was fixed, the mechanical properties were chosen so as to fulfill the optical requirements. Mechanical optimization of the structure was done using the Finite Element Method (FEM) using ANSYS 5.7. It was designed to have a 1μm/g of mechanical sensitivity. Thus, the designed accelerometer is expected to have an optical sensitivity of >4dB/g in a linear range with a seismic mass displacement of ±1μm.

FABRICATION & CHARACTERIZATION

ARROW-based optical accelerometers were fabricated using 450μm BESOI wafers as substrate. ARROW multilayer waveguide consist on a 2μm thermal silicon oxide (n=1.46 @ 0.633μm), a 0.38μm LPCVD silicon nitride (n=2.00 @ 0.633μm), waveguide core is obtained by PECVD (n=1.485 @ 0.633nm), which is 87.5% etched by Reactive Ion etching (RIE) so as to assure cross-section confinement. Process is followed by a passivation layer also obtained by PECVD, but with lower refractive index (n=1.465 @0.633μm) so as to avoid scattering from dust, that will cause an increase of the total losses. Accelerometer definition was done by ways of standard micromechanical technology **[9]**

The first step on any integrated optical device is to know if the simplest structure, that is, an isolated waveguide, has the expected behavior. Although it could seem that it is worthless since waveguides are far well known, it provides with information concerning insertion losses, attenuation, wavelength response and light confinement.

Figure 6. Total losses as function of the waveguide width for ARROW-A structures

Using end-fire coupling, losses in test waveguides integrated on the accelerometer chip with different width were measured. As can be seen in figure 6, losses sharply increase as waveguide gets narrower. However, for values above 8μm, a saturation value around of 3dB is obtained. It has to be taken into account that total losses not only include attenuation, but also insertion losses. By measuring two identical waveguides but with a different length, it was possible to measure the insertion losses, which are 2.5dB. It can be seen that the three segments of the waveguide in the optical accelerometer present the same losses, which is desirable since power loss is asked to vary due to misalignment, not due to different attenuation on the segments itself.
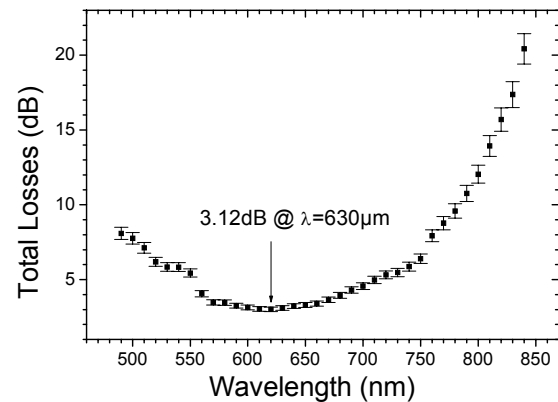

Figure 7. Total losses as function of the wavelength for ARROW-A structures

It is known that ARROW waveguides are wavelength-selective, that is, losses have a minimum at the working wavelength. Obviously, this is so if the cladding layers are properly tuned, both in refractive index and thickness. If there were any variation on any of these parameters, minimum losses will shift from the working wavelength. In figure 7, the total losses as a function of the wavelength for a waveguide with w=14μm can be observed. Measurements have a minimum at the expected λ=0.63μm,

confirming that the waveguide configuration works properly.

Once the optical properties of isolated waveguides were measured and their behavior was in agreement with the required specifications, the optical accelerometer was measured. Preliminary results of the output power as function of the gravitational field angle are presented in figure 8 for the 0-50º region. A trigonometric response is observed, which is consistent with a nearly linear behavior of the device due to acceleration changes.
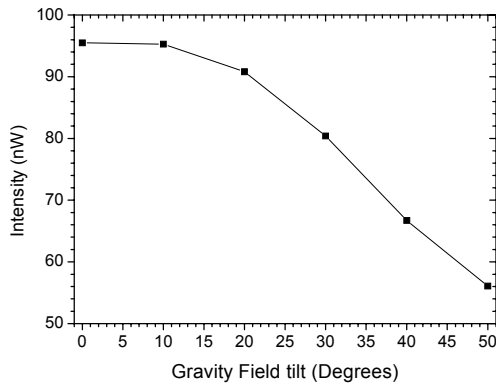
Figure 7. Output intensity in the optical accelerometer as function of the gravitational field tilt.

Summing up, a novel design of self-aligned stress-free quad beam optical accelerometer is presented. Standard TIR waveguides have been replaced by ARROW structures , which provides the device with larger linear region and much lower insertion losses. Simulations predict a sensitivity at the linear region >4dB/g. Experimental results confirm the correct behavior of the waveguides, with the expected minimum losses at the working wavelength, and the accelerometer, with a trigonometric response as a function of the wall tilt.

ACKNOWLEDGMENTS

REFERENCES

[1] F.Rudolf, A.Jornod, H.Leuthold. Precision Accelerometers with µg Resolution. Sens.& Act.A 21-23[297], 302. 1990.

[2] G.A.Macdonald. A Review of Low Cost Accelerometers for Vehicle Dynamics. Sens.& Act.A 21-23, 281-287. 1990.

[3] N.Yazdi, F.Ayazi, K.Najafi. Micromachined Inertial Sensors. Proced.IEEE 86[8], 1640-1659. 1998.

[4] J.M.López-Higuera, P.Mottier, A.Cobo, E.Ollier, M.A.Morante, C.Chabrol et al. Optical Fiber and Integrated Optics Accelerometers for Real Time Vibration Monitoring in Harsh Environments: In-Lab and in-Field Characterization. Europ.Works.Opt.Fib.Sens.(SPIE) 3483, 223-226. 1998.

[5] J.Kalenik, R.Pajak. A Cantilever Optical-fiber Accelerometer. Sens.& Act.A 68, 350-355. 1998.

[6] M.A.Duguay, Y.Kokubun, T.L.Koch. Antiresonant Reflecting Optical Waveguides in SiO_2-Si Multilayer Structures. Appl.Phys.Lett. 49[1], 13-15. 1986

[7] T.Baba, Y.Kokubun. Dispersion and Radiation Loss Characteristics of Antiresonant Reflecting Optical Waveguides-Numerical Results and Analytical Expressions. IEEE J.Quant.Elect. 28[7], 1689-1700. 1992.

[8] I.Garcés, F.Villuendas, J.A.Vallés, C.Domínguez, M.Moreno. Analysis of Leakage Properties and Guiding Conditions of Rib Antiresonant Reflecting Optical Waveguides. J.Light.Tech. 14[5], 798-805. 1996.

[9] K.Petersen. Silicon as a Mechanical Material. Proced.IEEE 70[5], 420-457. 1982. IEEE J.Quant.Elect. 28[7], 1689-1700. 1992.